

Continuum limit of quark number susceptibilities

Rajiv V. Gavai* and Sourendu Gupta†

Department of Theoretical Physics, Tata Institute of Fundamental Research, Homi Bhabha Road, Mumbai 400005, India

(Received 6 February 2002; revised manuscript received 15 March 2002; published 17 May 2002)

We report the continuum extrapolation of quark number susceptibilities in quenched QCD. Deviations from ideal gas behavior at temperature T increase as the lattice spacing is decreased from $1/4T$ to $1/8T$. The continuum extrapolation of the measured susceptibilities is 25% lower than the ideal gas values, and also 15% below the hard thermal loop (HTL) results. The off-diagonal susceptibility is several orders of magnitude smaller than the HTL results. We verify a strong correlation between the lowest screening mass and the susceptibility. We also show that the quark number susceptibilities give a reasonable account of the Wroblewski parameter, which measures the strangeness yield in a heavy-ion collision.

DOI: 10.1103/PhysRevD.65.094515

PACS number(s): 11.15.Ha, 12.38.Mh

I. INTRODUCTION

With the BNL Relativistic Heavy Ion Collider (RHIC) now in its second year of running, it is important to pin down lattice predictions for the high temperature phase of QCD. In this context, fully nonperturbative measurements of quark number susceptibilities [1–4] are important for four reasons. First, they are directly related to experimental measurements of event-to-event fluctuations in particle production [5]. Secondly, earlier results [3,4] showed a strong jump in the susceptibility across the phase transition, but indicated a significant departure from weak-coupling behavior, and it is important to check whether this persists into the continuum. Third, resummed perturbative computations of this quantity have now become available [6], thus making it possible to accurately test the importance of nonperturbative contributions to this quantity. Finally, with continuum extrapolated results in hand, one can address the question of whether the strangeness production seen in heavy-ion collisions can be quantitatively explained as a signal of the quark-gluon plasma.

We have recently presented systematic results for quark number susceptibilities in quenched QCD [3] as well as for QCD with two flavors of light dynamical quarks [4]. In these studies a large range of temperatures T was covered at a series of different quark masses m . These computations were done at a fixed cutoff with the lattice spacing $a = 1/4T$ while keeping the finite volume effects under control so that the thermodynamic limit could be taken reliably. There was a 3–5% difference between the quenched and dynamical computations. In this paper we examine the cutoff dependence of the quenched results and report their continuum (zero lattice spacing) limit.

The partition function of QCD with three quark flavors is

$$Z(T, \mu_u, \mu_d, \mu_s) = \int \mathcal{D}U \exp[-S(T)] \prod_{f=u,d,s} \det M(T, m_f, \mu_f), \quad (1)$$

where the temperature T determines the size of the Euclidean time direction, $S(T)$ is the gluonic part of the action and the determinants of the Dirac matrices M contain as parameters the quark masses m_f and the chemical potentials μ_f for each of the flavors $f = u, d, s$. We also define the chemical potentials $\mu_0 = \mu_u + \mu_d + \mu_s$, $\mu_3 = \mu_u - \mu_d$ and $\mu_8 = \mu_u + \mu_d - 2\mu_s$, which correspond to the diagonal flavor $SU(3)$ generators. Note that μ_0 is the usual baryon chemical potential and μ_3 is an isovector chemical potential.

Quark number densities are defined as

$$n_i(T, \mu_u, \mu_d, \mu_s) = \frac{T}{V} \frac{\partial \log Z}{\partial \mu_i} \quad (2)$$

and the susceptibilities as

$$\chi_{ij}(T, \mu_u, \mu_d, \mu_s) = \frac{T}{V} \frac{\partial^2 \log Z}{\partial \mu_i \partial \mu_j}, \quad (3)$$

where V denotes the spatial volume. The subscripts i and j are either of the index sets f or $\alpha = 0, 3$, and 8 . We lighten the notation by writing the diagonal susceptibilities χ_{ii} as χ_i . We determine the susceptibilities at zero chemical potential $\mu_f = 0$. In this limit, all $n_i(T) = 0$. Since we work with $m_u = m_d = m < m_s$, we also have $\chi_{03} = 0$.

Flavor off-diagonal susceptibilities such as

$$\chi_{ud} = \left(\frac{T}{V_3} \right) \langle \text{tr} M_u^{-1} M'_u \text{tr} M_d^{-1} M'_d \rangle \quad (4)$$

(M' is the derivative of M with respect to the chemical potential and M'' , below, is the second derivative) are given entirely in terms of the expectation values of disconnected loops. Since $m_u = m_d$, we obtain $\chi_{us} = \chi_{ds}$ with each defined by an obvious generalization of the formula above. Of the flavor diagonal susceptibilities we shall use

$$\chi_s = \left(\frac{T}{V_3} \right) [\langle (\text{tr} M_s^{-1} M'_s)^2 \rangle + \langle \text{tr} (M_s^{-1} M''_s - M_s^{-1} M'_s M_s^{-1} M'_s) \rangle]. \quad (5)$$

*Electronic address: gavai@tifr.res.in

†Electronic address: sgupta@tifr.res.in

$\chi_u = \chi_d$ are given by a generalization of this formula. Numerically, the simplest quantity to evaluate is the diagonal isovector susceptibility

$$\chi_3 = \frac{1}{2} \left(\frac{T}{V_3} \right) \langle \text{tr} (M_u^{-1} M_u'' - M_u^{-1} M_u' M_u^{-1} M_u') \rangle. \quad (6)$$

Two more susceptibilities are of interest. These are the baryon number and electric charge susceptibilities

$$\chi_0 = \frac{1}{9} (4\chi_3 + \chi_s + 4\chi_{ud} + 4\chi_{us})$$

and

$$\chi_q = \frac{1}{9} (10\chi_3 + \chi_s + \chi_{ud} - 2\chi_{us}). \quad (7)$$

Note that χ_0 is the baryon number susceptibility for three flavors of quarks. As a result, this expression differs from the iso-singlet quark number susceptibility for two flavors, defined in Ref. [1], both in overall normalization and by terms containing strangeness. In our numerical work we have chosen to use staggered quarks. Hence, to normalize to one flavor of continuum quarks and compensate for fermion doubling on the lattice, we have to multiply each of the traces in Eqs. (4)–(6) by a factor of 1/4.

The quark mass appears in two logically distinct places—first in the operators which define the susceptibilities in Eqs. (4)–(6), and secondly in the determinant in the partition function of Eq. (1) which defines the weight for the averaging of these operators. The first defines a valence quark mass and the second the sea quark mass. In this paper we adopt the quenched approximation, whereby the determinants in Eq. (1) are set equal to unity. However, we shall vary the valence quark masses. As shown earlier, unquenching the sea quarks changes results by 3–5% [3,4].

Note that all the flavor off-diagonal susceptibilities are exactly zero in an ideal gas. We shall denote by χ_{FFT}^3 the ideal gas value for χ_3 . On an $N_t \times N_s^3$ lattice with N_c colors and lattice spacing a , we find

$$a^2 \chi_{\text{FFT}}^3 = \frac{N_c}{2N_t N_s^3} \sum_p \left\{ D^{-2} \sin^2 p_0 \cos^2 p_0 + D^{-1} \left(\sin^2 p_0 - \frac{1}{2} \right) \right\}, \quad (8)$$

where the spectrum of momenta is $p_0 = (2\pi/N_t)(n+1/2)$ with $0 \leq n < N_t$ and $p_i = 2\pi n/N_s$ with $0 \leq n < N_s$, and $D = (ma)^2 + \sum_\mu \sin^2 p_\mu$. For $N_t = 4$ the second term in the above formula vanishes, and we recover the expression in Ref. [4]. For a given m/T_c and T/T_c , the value of the quark mass in lattice units is

$$ma = \left(\frac{1}{N_t} \right) \left(\frac{m}{T_c} \right) \left(\frac{T_c}{T} \right). \quad (9)$$

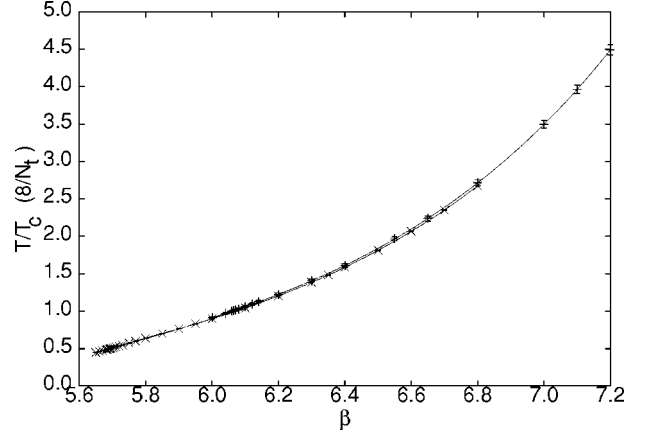


FIG. 1. The temperature for any value of N_t for a given coupling β . Crosses denote data for $N_t=4$ lattices and pluses for $N_t=8$ lattices. The scale has been set by a corrected QCD 2-loop formula [9]. The difference between the two sets of data is a measure of scale breaking by residual power-law corrections and is negligible within statistical errors.

The formula in Eq. (8) is normalized such that there is exactly one copy of each flavor of quarks. The values of χ_s, χ_0 and χ_q for an ideal gas can then be simply obtained as linear combinations of χ_{FFT}^3 for different valence quark masses.

II. LATTICE RESULTS

We have previously reported measurements of χ_3 in quenched QCD with 4 time slices ($N_t=4$) at temperatures of $1.1T_c, 1.25T_c, 1.5T_c, 2T_c$, and $3T_c$ [2]. We have extended these measurements to higher temperatures through two simulations on 4×20^3 lattices at $\beta=6.6$ and 6.7 . These correspond to temperatures of $4.13T_c$ and $4.7T_c$. All these computations are performed at fixed bare quark masses of $m/T_c = 0.03, 0.3, 0.5, 0.75$ and 1 (the data for $m/T_c = 0.5$ are new).

The continuum limit has been taken by going to several smaller lattice spacings. One set of computations is performed with a lattice spacing $a=1/6T$ which is 33% smaller than the lattice spacing used earlier. We have taken data on 6×20^3 lattices at $\beta=6.0625, 6.3384$, and 6.7 corresponding to $T/T_c = 1.333, 2$, and 3.133 , and on a 6×24^3 lattice at $\beta=6.8$ corresponding to $T/T_c = 3.532$. One further computation was made on an 8×18^3 lattice at $\beta=6.55$. This corresponds to $T/T_c = 2$ with lattice spacing $a=1/8T$. The quark mass m/T_c is kept independent of a and T , and hence ma decreases with increasing T at fixed N_t or with increasing N_t at fixed T according to Eq. (9).

The lattice scale has been set using the plaquette measurements of Ref. [8] and the analysis performed in Ref. [9]. The conversion of β to T using data for $N_t=4$ and 8 give the two curves in Fig. 1. The difference between the two curves is within the statistical uncertainty of 5% on the scale assignment. There is the same degree of statistical uncertainty in the bare quark masses and in all other scales. We shall not display this inherent scale uncertainty in the measurements, but it should be kept in mind.

The simulations have been performed with a Cabibbo-

Marinari pseudo-heatbath technique with 3 $SU(2)$ subgroups updated on each hit. An initial 1000 sweeps have been discarded for thermalization. On the $N_t \leq 6$ lattices we have used 80 configurations separated by 1000 sweeps for the measurements. On the $N_t = 8$ lattice we have used 55 configurations separated by 500 sweeps.

We have previously checked that the spatial lattice size $L = N_s a$ is quite irrelevant to the values of χ measured as long as it is sufficiently large compared to the inverse pion mass [2,4]. In fact, at all the couplings and quark masses we have used, $m_\pi L \geq 5$. The most important other constraint on L comes from the requirement that it should be large enough to prevent spatial deconfinement [7]. This is ensured by taking $N_s/N_t > T/T_c$ in all our simulations.

The traces are evaluated by the usual stochastic technique

$$\text{Tr} A = \frac{1}{2N} \sum_{i=1}^N R_i^\dagger A R_i, \quad (10)$$

where R_i are a set of N uncorrelated vectors with components drawn independently from a Gaussian ensemble with unit variance. Each vector has three color components at each site of the lattice. Since we use a half lattice version of the Dirac operator for staggered fermions, the number of components of each vector R_i is one and a half times the number of lattice points. $(\text{Tr} A)^2$ is obtained by dividing the set of R_i into disjoint blocks, constructing $\text{Tr} A$ in each block, taking all possible distinct pairs of such estimates, multiplying them and then averaging over the pairs. For $N_t = 4$ it is possible to get accurate results with $N \approx 10$, although we have chosen to use $N = 80$ for each gauge configuration [4].

It is easy to check that the variance of the estimator above is proportional to $\text{Tr}(A^2)$. Since the diagonal element of the fermion matrix is proportional to the quark mass ma , whereas the off-diagonal elements are bounded by unity, with increasing T or decreasing a , $\text{Tr} A$ decreases linearly, while its variance remains constant. Hence, for sufficiently small ma the number of vectors has to increase quadratically with ma . We found that $N = 100$ was sufficient for $N_t = 8$ at $T = 2T_c$, although at larger N_t or T significantly larger values of N_v are needed. A further numerical problem arises from the cancellation of the two matrix elements which give χ_3 [see Eq. (6)]. While increasing N_t and keeping the physical size of the lattice fixed, each of these terms increases quadratically but mutually cancel to give a number which decreases quadratically with N_t . At fixed word length, this implies a reduction in accuracy by a factor of N_t^4 . As a result of the interplay of these two problems, we were unable to obtain statistically significant results for $N_t = 10$ using double precision arithmetic.

In Fig. 2 we show our measurements of χ_3 at fixed temperature as the lattice spacing ($a \propto 1/N_t$) is varied. Since we use staggered quarks in this measurement, it is expected that for small enough lattice spacings the cutoff effects would vanish as a^2 . As the figure shows, such fits are consistent with the data for $N_t = 4, 6$, and 8 and all quark masses we have used in our measurements at $2T_c$. In the same figure

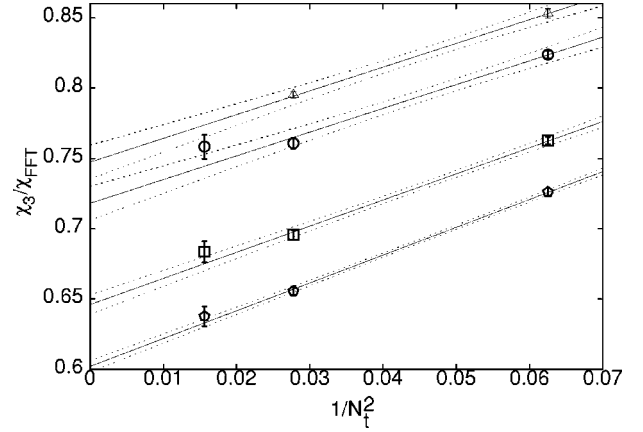


FIG. 2. $\chi_3/\chi_{\text{FFT}}^3$ at $T=2T_c$ shown as a function of $a^2 \propto 1/N_t^2$ for $m/T_c = 0.03$ (circles), 0.75 (boxes), and 1.00 (pentagons). Continuum extrapolations are shown (full lines) along with the one sigma error bands computed using the full covariance matrix (dotted lines). Also shown are data for $T=3T_c$ and $m/T_c = 0.03$ (triangles) along with the best fit of $T=2T_c$ translated up to pass through the measured points. In the range of T and m explored, the slopes do not seem to depend upon either of these parameters.

we also show the data taken at $3T_c$ on the lattices with $N_t = 4$ and 6 [21]. As demonstrated in the figure, the slope of the a^2 dependence does not change from $2T_c$. Similar results hold at other temperatures. As a result the $N_t = 6$ measurements set an upper bound to the continuum limit of $\chi_3/\chi_{\text{FFT}}^3$. Also, since the slope does not depend on the parameters T/T_c and m/T_c (within statistical errors and in the range of parameters explored), the continuum limit can be obtained by subtracting $(0.047 \pm 0.006)\chi_{\text{FFT}}^3$ from the measurement of χ_3 on lattices with $N_t = 6$.

As noted before, the second term in the sum on the right of Eq. (8) vanishes for $N_t = 4$. This accident occurs only for $N_t = 4$, and for all other values of N_t this term contributes a nonvanishing value. It is easy to see that in the limit $N_t \rightarrow \infty$ this term contributes to the leading part of χ_{FFT}^3 . Whether this leads to a systematic uncertainty in the a^2 extrapolation to zero lattice spacing needs to be checked by future computations with larger N_t .

Our results for the dependence of $\chi_3/\chi_{\text{FFT}}^3$ on T/T_c at different quark masses for $N_t = 4$ and 6 are shown in Fig. 3. For $N_t = 4$ the data points at $T/T_c > 4$ are new; although data was taken for various values of m/T_c , only the highest and lowest are shown in the figure for clarity. Also shown is the continuum extrapolation using the method outlined above (the extrapolated numbers are also collected in Table I). The continuum extrapolation of χ_3 lies well below the ideal gas limit even at temperatures as high as $3.5T_c$. Closer to T_c the value of χ_3 dips further below the ideal gas limit. We have also measured the off-diagonal susceptibility χ_{ud} . As already seen for $N_t = 4$ this is consistent with zero even for $N_t = 6$. In Table I we show that the continuum limit of χ_{ud} also vanishes within errors of $10^{-7}T^2$. It is therefore much smaller than the 3-loop perturbative result given in Ref. [6].

Note that the continuum limit of our measurements lie about 25% below the ideal gas result. They also differ sig-

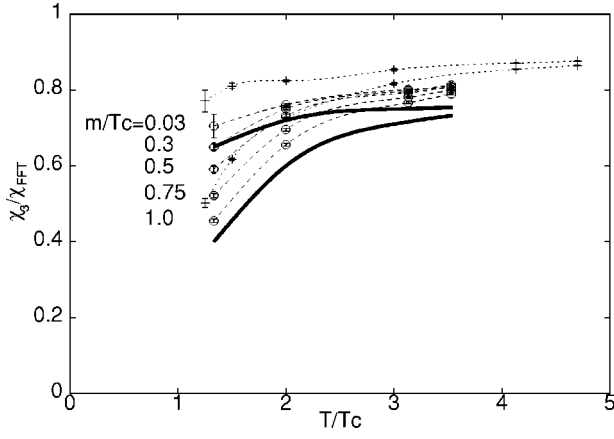


FIG. 3. The ratio $\chi_3/\chi_{\text{FFT}}^3$ in quenched QCD, shown as a function of T for the values of m/T_c indicated. Pluses denote data for lattice spacing $a=1/4T$ and circles for $a=1/6T$. The lines are cubic splines through the data. For $a=1/4T$ (dotted lines) and the continuum extrapolation (thick lines) only $m/T_c=0.03$ and 1.0 are shown for clarity.

nificantly from HTL as well as the skeleton graph resummed results of Ref. [6]. At $T=3T_c$, HTL predicts $\chi_3/\chi_{\text{FFT}}^3=0.90-0.94$ on varying the scale of α_s between πT and $4\pi T$, and the resummed computation gives $\chi_3/\chi_{\text{FFT}}^3=0.95-0.97$. Our measurement shows $\chi_3/\chi_{\text{FFT}}^3=0.75$ at $3T_c$ (see Table I). A second computation of the HTL result is available for $N_f=2$ [10]. Since this agrees with the HTL result of Ref. [6] for $N_f=2$, we believe the HTL result for $\chi_3/\chi_{\text{FFT}}^3$ is under control. There is thus a genuine discrepancy between these lattice results and existing perturbative computations.

The quark number susceptibilities are closely related to the screening correlator of a one-link separated quark bilinear operator which corresponds to a ρ meson at zero temperature. The $T>0$ transfer matrix of the problem mixes this with a quark bilinear that corresponds to the π [11]. We have earlier shown evidence for $N_f=4$ that χ_3 is closely related to the only known nonperturbative quantity among the screening correlators, that is the screening mass M_S coming from the two degenerate correlators that descend from the π and σ operators of the zero temperature theory [4]. In view of the strongly nonperturbative character of χ_3 , as revealed by the comparison with HTL and resummation explained above, examining this correlation in the continuum becomes more sig-

TABLE I. Results for the continuum limit of quark number susceptibility in quenched QCD. We have taken $m_s/T_c=1$ as appropriate to full QCD. For $T>3T_c$ mass effects are small and all the nonvanishing susceptibilities tend to the same fraction of their free field values. Our $N_f=4$ results indicate that at higher T the ratios χ/χ_{FFT} are reasonably flat.

T/T_c	$\chi_3/\chi_{\text{FFT}}^3$	χ_{ud}/T^2	$\chi_s/\chi_{\text{FFT}}^s$	$\chi_0/\chi_{\text{FFT}}^0$	$\chi_q/\chi_{\text{FFT}}^q$
1.333	0.65 (4)	$(2\pm 4)\times 10^{-6}$	0.40 (1)	0.61 (2)	0.63 (3)
2.000	0.72 (1)	$(-1\pm 2)\times 10^{-7}$	0.60 (1)	0.69 (1)	0.70 (1)
3.133	0.75 (1)	$(-1\pm 1)\times 10^{-7}$	0.71 (1)	0.74 (1)	0.74 (1)
3.532	0.75 (1)	$(1\pm 2)\times 10^{-7}$	0.74 (1)	0.75 (1)	0.75 (1)

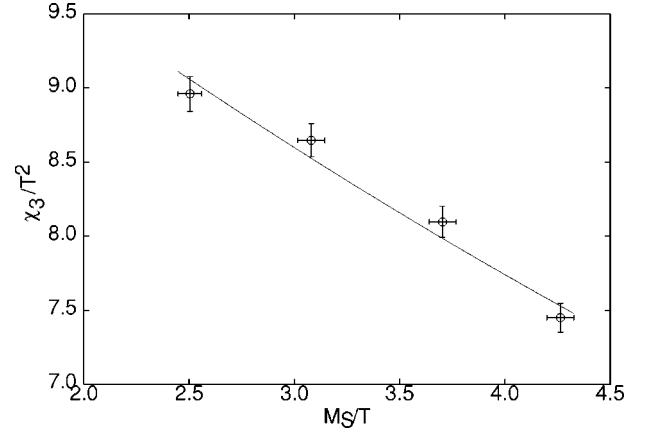


FIG. 4. Correlation between the screening mass in the scalar/pseudoscalar sector M_S and the quark number susceptibility χ_3 at $2T_c$. The measurements have been made on a 8×18^3 lattice at a series of quark masses. An exponential fit to the data, following [4], is also shown.

nificant. In Fig. 4 we show data obtained on 8×18^3 lattices which indicate that this correlation survives into the continuum.

III. STRANGENESS

Measurements of hadron yields in relativistic heavy-ion collisions have been analyzed extensively [12,13] and the observed enhancement of strangeness has been claimed to be evidence for quark-gluon plasma formation. The chemical composition is observed at the hadron freezeout temperature, which has been found to be very close to the value of T_c in full QCD. It has been argued that this chemical composition cannot arise due to hadronic rescattering [14]. It would be interesting if it could be directly determined whether or not the composition is characteristic of the plasma for $T\geq T_c$. We argue below that this question can be answered by a lattice QCD measurement such as we have presented above.

The quantity which seems to be directly connected to lattice measurements is the Wroblewski parameter [15] λ_s which measures the ratio of newly created primary strange to light quarks

$$\lambda_s = \frac{2\langle s\bar{s} \rangle}{\langle u\bar{u} + d\bar{d} \rangle}. \quad (11)$$

A fluctuation-dissipation theorem relates the rate of production of quark pairs by the plasma in equilibrium to the imaginary part of the full complex quark number susceptibilities [16]. If the inverse of the characteristic time scales of the QCD plasma are not close to the typical energy scales for the production of strange and lighter quarks, then the ratio of their production rates is just the ratio of the static susceptibilities that we have measured. Then, if the observed chemical composition is created in equilibrium, we should have

$$\lambda_s = \frac{2\chi_s}{\chi_u + \chi_d} \approx \frac{\chi_s}{\chi_u}, \quad (12)$$

where the last equality holds in the limit of equal u and d quark masses. These susceptibilities have to be evaluated on the lattice at the temperature and chemical potential μ_0 relevant to the collision. However, it has been shown recently [17] that λ_s is insensitive to μ_0 for SPS and RHIC energies. Furthermore a lattice measurement shows that the screening mass M_S does not change rapidly with increasing chemical potential [18]. Then, in view of the correlation between M_S and χ shown in Fig. 4, we do not expect rapid changes with chemical potential in the ratio above. Both these arguments show that as a first approximation one can take the ratio in Eq. (12) at zero chemical potential.

From our measurements of χ reported here, we can form the lattice ‘‘prediction’’ of λ_s created in the plasma at T_c . This requires an extrapolation of our measurements to $T = T_c$. Since we have measurements at four different values of T/T_c , we perform this extrapolation through a variety of three parameter fits to the data, as well as a linear extrapolation through the data at $T/T_c = 4/3$ and 2. The forms that we have used are

$$\begin{aligned}\chi(T/T_c) &= a_1 + b_1 \left(\frac{T}{T_c} \right), \\ \chi(T/T_c) &= a_2 + \left(\frac{T}{T_c} \right) \left[b_2 + c_2 \left(\frac{T}{T_c} \right) \right], \\ \chi(T/T_c) &= a_3 + \left(\frac{T}{T_c} \right) \left[b_3 + c_3 \log \left(\frac{T}{T_c} \right) \right], \\ \chi(T/T_c) &= a_4 + \log \left(\frac{T}{T_c} \right) \left[b_4 + c_4 \log \left(\frac{T}{T_c} \right) \right].\end{aligned}\quad (13)$$

The statistical errors in the extrapolation come from the variation of the fit parameters within the error bounds of the measurements, and estimates of systematic uncertainties in the extrapolation come from comparison of the different extrapolations. For χ_u we have used data taken for $m/T_c = 0.03$, which is light enough for this purpose. Since scaled quantities feel the smallest correction for unquenching [4], we take χ_s to correspond to $m/T_c = 1$, which is appropriate to full QCD. In Fig. 5 the resultant prediction is compared with the data collected in Refs. [13,17]. The central value of the lattice prediction and the statistical error bar shown in the figure are from the linear extrapolation. The systematic error interval shown is the spread of the best fit value from the different fits.

It can be seen that there is a fair agreement with the data. However, this is subject to several assumptions.

(1) The foremost assumption is that the characteristic time scales of the plasma are not close to the inverse energy scale of the production processes. It is not possible to test this assumption in an Euclidean computation. However, it has been suggested that these characteristic time scales could be observed in real or virtual photon production as spikes in the spectrum [19]. If these are seen and they lie in the energy range for the production, the assumption would be falsified.

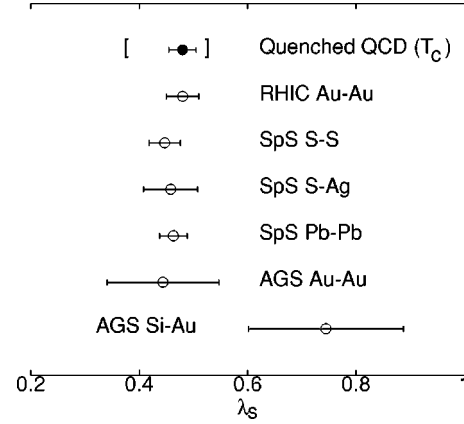


FIG. 5. The Wroblewski parameter λ_s obtained from various experimental measurements, compared with the value obtained from the lattice measurements reported here. For the lattice result the error bar comes from statistical errors and the bracketed interval is a measure of systematic uncertainties in the extrapolation to T_c .

(2) Another important assumption is that chemical equilibration takes place in the plasma. If chemical equilibrium is not achieved but the light degrees of freedom achieve energy equipartition, then the effective temperature could be higher.

(3) We have assumed slow variation of the ratio χ_s/χ_u with chemical potential. While this seems to be a reasonable estimate in view of the results of Refs. [17,18] and our own observations about the relation between the lowest screening mass and the susceptibilities, one should keep in mind possible changes in the ratio due to violation of this assumption.

(4) Our continuum results are obtained in quenched QCD, whereas the data corresponds to full QCD. As mentioned already, we have taken $m/T_c = 1$, as appropriate to full QCD, in order to correct for this. However, an additional 5–10% shift in our results could arise when unquenching [4]. This is not shown in Fig. 5.

(5) Our measurements are made away from T_c and extrapolated down to this temperature. Clearly systematic errors dominate this extrapolation. In principle this can be corrected by a computation made directly at T_c . However, due to the enormous cost of extracting physical quantities at T_c , we postpone this to the time when we attempt a full QCD simulation.

It might seem surprising that λ_s corresponds to the chemical composition at T_c . However, a moment’s thought shows that this is entirely in accord with the assumption of chemical equilibrium. Even if the system is thermalized at a much higher temperature, it remains in equilibrium until it reaches T_c . Departure from equilibrium as the system cools through the transition is unlikely, and if it occurs, should have a visible signature such as the formation of a disoriented chiral condensate [20]. In the absence of such phenomena, if λ_s does not correspond to the chemistry at T_c , then the second assumption above would be demonstrated to be false. Also, with increasing ion energy the system moves closer to zero baryon number, as seen at RHIC. This makes our third assumption better at the RHIC and the CERN Large Hadron Collider (LHC). The fourth assumption can be removed by a computation with full QCD. Such a computation is planned,

where also the final assumption can be removed, and will be reported elsewhere.

IV. SUMMARY

In summary, we have presented new and precise results on quark number susceptibilities over a wide range of temperatures and quark masses obtained at different lattice spacings a in the high temperature phase of QCD. The main aim of this study was to obtain the continuum extrapolation of these susceptibilities. As shown in Fig. 2, the expected scaling of the results as a^2 is consistent with the data on lattices with a ranging from $1/4T$ to $1/8T$. The coefficient of the a^2 term seems to be statistically independent of the quark mass and temperature in the range where we have taken our measurements, thus allowing us to extrapolate the lattice measurements to the continuum. This extrapolation is shown in Fig. 3 and Table I.

There is a strong discrepancy between the continuum ex-

trapolated lattice results and HTL computations for these quantities—varying between about 15% at the highest T to somewhat more at smaller T . The off-diagonal susceptibility χ_{ud} is zero, in contrast to the HTL results of Ref. [6]. There is a somewhat larger discrepancy between the continuum extrapolated lattice results and the skeleton graph resummed results. The conjecture that there is a strong nonperturbative component to the quark number susceptibilities is supported by an observed strong correlation between the smallest quark bilinear screening mass M_S and the susceptibility χ_3 (Fig. 4).

It is interesting to note that the continuum extrapolated results for the strange and light quark susceptibilities can be used to give a surprisingly good description of the chemical composition of hadrons at freezeout in the CERN Super Proton Synchrotron (SPS) and RHIC experiments (Fig. 5). This has to be treated as a preliminary estimate due to the many caveats which we have listed, and some of which we plan to check in future lattice measurements.

-
- [1] S. Gottlieb *et al.*, Phys. Rev. Lett. **59**, 2247 (1987).
 - [2] R.V. Gavai *et al.*, Phys. Rev. D **40**, 2743 (1989); C. Bernard *et al.*, *ibid.* **54**, 4585 (1996); S. Gottlieb *et al.*, *ibid.* **55**, 6852 (1997).
 - [3] R.V. Gavai and S. Gupta, Phys. Rev. D **64**, 074506 (2001).
 - [4] R.V. Gavai, S. Gupta, and P. Majumdar, Phys. Rev. D **65**, 054506 (2002).
 - [5] M. Asakawa, U. Heinz, and B. Müller, Phys. Rev. Lett. **85**, 2072 (2000); S. Jeon and V. Koch, *ibid.* **85**, 2076 (2000); D. Bower and S. Gavin, Phys. Rev. C **64**, 051902 (2001); S. Jeon, V. Koch, K. Redlich, and X.N. Wang, Nucl. Phys. **A697**, 546 (2002).
 - [6] J.-P. Blaizot, E. Iancu, and A. Rebhan, Phys. Lett. B **523**, 143 (2001).
 - [7] S. Datta and S. Gupta, Phys. Lett. B **471**, 382 (2000).
 - [8] G. Boyd *et al.*, Nucl. Phys. **B469**, 419 (1996).
 - [9] S. Gupta, Phys. Rev. D **64**, 034507 (2001).
 - [10] P. Chakraborty, M.G. Mustafa, and M.H. Thoma, hep-ph/0111022.
 - [11] S. Gupta, Phys. Rev. D **60**, 094505 (1999).
 - [12] P. Braun-Munzinger *et al.*, Phys. Lett. B **465**, 43 (1999); J. Letessier and J. Rafelski, Nucl. Phys. **A661**, 97c (1999).
 - [13] F. Becattini *et al.*, Phys. Rev. C **64**, 024901 (2001).
 - [14] U. Heinz, J. Phys. G **25**, 263 (1999); R. Stock, Phys. Lett. B **456**, 277 (1999).
 - [15] A. Wroblewski, Acta Phys. Pol. B **16**, 379 (1985).
 - [16] P.C. Martin, in *Many Body Physics*, Proceedings of the 1967 Les Houches School, edited by C. DeWitt and R. Balian (Gordon and Breach, New York, 1968); W. Marshall and S.W. Lovesey, *Theory of Thermal Neutron Scattering* (Oxford University Press, London, 1971); A.L. Fetter and J.D. Walecka, *Quantum Theory of Many-particle Systems* (McGraw-Hill, New York, 1971).
 - [17] J. Cleymans, hep-ph/0201142.
 - [18] S. Choe *et al.*, Nucl. Phys. B (Proc. Suppl.) **106**, 402 (2002).
 - [19] H.A. Weldon, Nucl. Phys. **A525**, 405c (1991); S. Gupta, *ibid.* **A566**, 69c (1994).
 - [20] K. Rajagopal and F. Wilczek, Nucl. Phys. **B404**, 577 (1993).
 - [21] Due to the previously mentioned systematic uncertainty in scale setting, this simulation at $N_t=6$ corresponds to $T/T_c = 3.133 \pm 0.157$ and hence can be compared to the measurement at $3T_c$ with $N_t=4$.